Chinese Journal of Natural Medicines

New acylphloroglucinol–sesquiterpenoid adducts with antiviral activities from *Dryopteris atrata*

Jihui Zhang, Jinghao Wang, Wei Tang, Xi Shen, Jinlin Chen, Huilin Ou, Qianyi Situ, Yaolan Li, Guocai Wang, Yubo Zhang, Nenghua Chen

Citation: Jihui Zhang, Jinghao Wang, Wei Tang, Xi Shen, Jinlin Chen, Huilin Ou, Qianyi Situ, Yaolan Li, Guocai Wang, Yubo Zhang, Nenghua Chen, New acylphloroglucinol–sesquiterpenoid adducts with antiviral activities from *Dryopteris atrata*, Chinese Journal of Natural Medicines, 2025, 23(3), 377–384. doi: 10.1016/S1875–5364(25)60839–9.

View online: https://doi.org/10.1016/S1875–5364(25)60839–9

Chinese Journal of Natural Medicines 23 (2025) 377-384

Contents lists available at ScienceDirect

Chinese Journal of Natural Medicines

journal homepage: www.cjnmcpu.com/

Original article

New acylphloroglucinol-sesquiterpenoid adducts with antiviral activities from *Dryopteris atrata*

Jihui Zhang[a,Δ], Jinghao Wang[b,c,Δ], Wei Tang[a,Δ], Xi Shen[d], Jinlin Chen[a], Huilin Ou[a], Qianyi Situ[a], Yaolan Li[a], Guocai Wang[a,c,*], Yubo Zhang[c,d,*], Nenghua Chen[b,c,*]

[a] *Institute of Traditional Chinese Medicine & Natural Products, Guangdong Province Key Laboratory of Pharmacodynamic Constituents of TCM and New Drugs Research, College of Pharmacy, Jinan University, Guangzhou 510632, China*

[b] *Department of Pharmacy, The First Affiliated Hospital, Jinan University, Guangzhou 510630, China*

[c] *The Guangzhou Key Laboratory of Basic and Translational Research on Chronic Diseases, Jinan University, Guangzhou 510630, China*

[d] *Guangdong Clinical Translational Center for Targeted Drug, Department of Pharmacology, School of Medicine, Jinan University, Guangzhou 510632, China*

ARTICLE INFO

Article history:
Received 26 December 2023
Revised 13 May 2024
Accepted 17 May 2024
Available online 20 April 2025

Keywords:
Dryopteris atrata
Acylphloroglucinol-sesquiterpenoid adducts
Structural elucidation
Antiviral activities

ABSTRACT

Seven novel acylphloroglucinol-sesquiterpenoid adducts, designated as dryatraols J–P (**1**–**7**), were isolated from the rhizomes of *Dryopteris atrata* (Wall. ex Kunze) Ching. The structures, including absolute configurations, were elucidated using comprehensive spectroscopic data, calculated ^{13}C Nuclear Magnetic Resonance-Diastereotopic Probability Assignment Plus (^{13}C NMR-DP4+) probability analysis, and ECD calculations. These structures represent a rare subclass of carbon skeleton of acylphloroglucinol-sesquiterpenoid adducts with a furan ring connecting the acylphloroglucinol and sesquiterpenoid moieties. Notably, compounds **1**–**6** are the first reported examples of acylphloroglucinol-sesquiterpenoid adducts with dimeric acylphloroglucinol incorporated into the aristolane- or rulepidanol-type sesquiterpene, while compound **7** features a hydroxylated monomeric acylphloroglucinol motif. A preliminary evaluation of their antiviral activities revealed that compounds **1**–**6** exhibited more potent activities against respiratory syncytial virus (RSV) with IC_{50} values ranging from 0.75 to 3.12 μmol·L^{-1} compared to the positive control (ribavirin).

1. Introduction

Phloroglucinols constitute a significant class of natural products, characterized by their chemical diversity and extensive range of biological activities. These compounds are widely distributed across land plants, marine organisms, and microorganisms [1-2]. Within the genus *Dryopteris*, phloroglucinols are considered characteristic constituents and can be categorized into two primary subclasses: oligomeric acylphloroglucinols and acylphloroglucinol-terpenoid adducts [3]. Comprehensive studies on *Dryopteris* species have led to the characterization of over 200 phloroglucinols. Although acylphloroglucinol-terpenoid adducts represent a minority among these compounds, they have garnered increasing attention due to their intriguing structures and notable antiviral, antifungal, antibacterial, and anti-inflammatory properties [3-7].

In our previous investigations of the genus *Dryopteris* (*D. championiiand*, *D. crassirhizoma*, and *D. atrata*), we sought structurally diverse and bioactive acylphloroglucinol-terpenoid adducts. These studies resulted in the isolation and identification of several unique skeletal structures with potent bioactivities[4, 8-9]. Continuing our research on the rhizomes of *D. atrata*, we isolated seven new acylphloroglucinol-sesquiterpenoid adducts, representing a less common subclass of carbon architecture featuring a furan ring as the coupling pattern (Fig. 1). Compounds **1**–**6** are noteworthy dimeric acylphloroglucinol-sesquiterpenoid adducts, while compound **7** is characterized by a hydroxylated monomeric acylphloroglucinol unit. These isolates were evaluated for their antiviral activities against herpes simplex virus type 1 (HSV-1) and respiratory syncytial virus (RSV). Significantly, compounds **1**–**6** demonstrated superior antiviral activities against RSV compared to the positive control (ribavirin), with IC_{50} values ranging from 0.75 to 3.12 μmol·L^{-1}. This study details the isolation process, structural characterization, and antiviral evaluation of these compounds.

2. Result and Discussion

The NMR spectra of compounds **1**–**6** exhibited two analogous sets of signals in an approximate ratio of 6∶1. This observation is attributed to the keto-enol tautomerization of the enolizable 1,3-diketone system present in the filicinic acid moiety, a phenomenon previously documented [4]. For the purposes of this study, only the major isomer of each compound is described.

The molecular formula of compound **1** was established as $C_{34}H_{42}O_9$ based on the high-resolution electrospray ionization mass spectrometry (HR-ESI-MS) ion peak at *m/z* 595.2895

* Corresponding author.
E-mail addresses: twangguocai@jnu.edu.cn (G. Wang); ybzhang99@126.com (Y. Zhang); chennenghua@jnu.edu.cn (N. Chen)
Δ These authors contributed equally to this work.

https://doi.org/10.1016/S1875-5364(25)60839-9

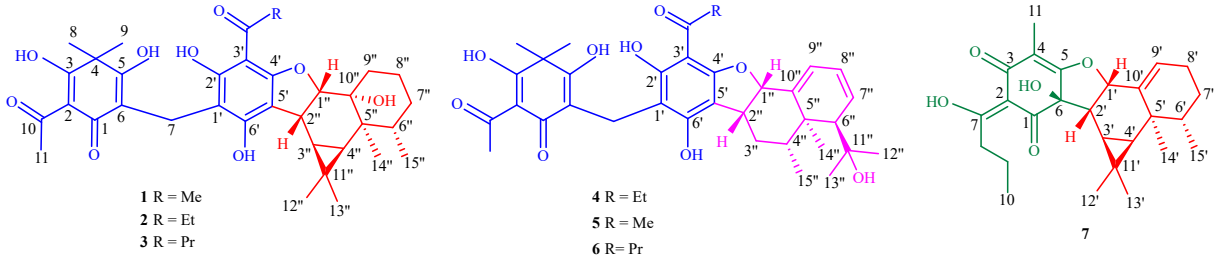

Fig. 1 Structures of compounds **1**–**7**.

$[M + H]^+$ (Calcd. for $C_{34}H_{43}O_9$, 595.2902) and the ^{13}C NMR data, indicating fourteen double bond equivalents. The ^1H nuclear magnetic resonance (NMR) spectrum (Table 1) revealed four distinctive hydroxyl groups [δ_H 18.51, 15.33, 11.30 and 9.91 (each 1H, s)], two shielded methine protons [δ_H 0.52 and 0.49 (each 1H, d, J = 10.1 Hz)], and eight methyl groups [δ_H 2.69, 2.56, 1.49, 1.48, 1.46, 1.08 and 1.02 (each 3H, s), and 0.87 (3H, d, J = 6.9 Hz)]. The ^{13}C NMR data, supported by heteronuclear single quantum coherence (HSQC) and distortionless enhancement by polarization transfer (DEPT) experiments, exhibited thirty-four carbon resonances attributed to seventeen non-protonated carbons (including thirteen sp^2 at δ_C 203.9, 202.7, 199.5, 188.0, 172.2, 161.0, 160.6, 160.5, 113.9, 111.8, 108.9, 106.7 and 101.5, and one sp^3 at δ_C 44.7), five methines (one oxygenated at δ_C 91.9), four methylenes (one at δ_C 17.0), and eight methyls (four at δ_C 30.6, 29.2, 25.0, 24.7). Detailed analysis of the aforementioned 1D NMR data indicated the presence of a norflavaspidic acid moiety (fragment Ⅰ) in **1** [10]. Subsequently, careful comparison of the remaining fifteen resonances (fragment Ⅱ) demonstrated good agreement with those of an aristolane-type sesquiterpene of 10-hydroxyaristolan-9-one [11]. Considering this information, it was deduced that compound **1** was an adduct composed of a dimeric acylphloroglucinol and an aristolane–type sesquiterpene.

The assignment of fragments I and Ⅱ, as well as the coupling pattern, was further corroborated through analysis of the 2D NMR data (Fig. 2). In the heteronuclear multiple bond correlation (HMBC) spectrum, correlations from H_3-11 (δ_H 2.69) to C-2 (δ_C 108.9)/C-10 (δ_C 203.9) and from H_3-8′ (δ_H 2.56) to C-3′ (δ_C 101.5)/C-7′ (δ_C 202.7) indicated that both substituents in the side chains of fragment Ⅰ were acetyl groups, connected to C-2 and C-3′, respectively. This supported the identification of fragment Ⅰ as a norflavaspidic acid AA moiety. Furthermore, comparison revealed that the primary distinction between fragment Ⅱ and 10-hydroxyaristolan-9-one was the presence of two methine carbons (δ_C 91.9, C-1″ and δ_C 34.3, C-2″) in **1**, replacing one ketone group (δ_C 215.9, C-9) and one methylene carbon (δ_C 34.5, C-8) in 10-hydroxyaristolan-9-one. It was deduced that C-8/C-9 in 10-hydroxyaristolan-9-one were replaced by C-1″/C-2″ in **1**, serving as the fused positions linking fragment Ⅰ. This deduction was confirmed by the HMBC correlations from H-2″ (δ_H 3.49) to C-4′ (δ_C 161.0)/C-5′ (δ_C 113.9)/C-6′ (δ_C 160.6) and ^1H-^1H COSY correlation of H-1″ (δ_H 4.28) and H-2″, along with the molecular formula information and chemical shifts of C-4′/C-1″ indicating an oxygen bridge between C-4′ and C-1″. Consequently, a furan ring was identified as the coupling pattern linking fragments Ⅰ and Ⅱ, thereby determining the planar structure of **1**.

The relative configuration of **1** was elucidated through analysis of nuclear overhauser effect spectroscopy (NOESY) experiment data. In the NOESY spectrum (Fig. 3), cross peaks between H_3-14″ (δ_H 1.08) and H-4″ (δ_H 0.49)/H_3-15″ (δ_H 0.87) indicated their positioning on the same side, arbitrarily assigned as α-orientation. Then, the NOE correlation of H-1″ (δ_H 4.28) and H-6″ (δ_H 2.32) suggested HO-10″ and H_3-14″ shared the same orientation. Additionally, the correlation between H-2″ (δ_H 3.49) and H_3-13″ (δ_H 1.49) revealed that H-1″ and H-2″ were β-oriented. These observations established the relative stereochemistry. The absolute configuration of compound **1** was determined through quantum-chemical electronic circular dichroism (ECD) calculations. As illustrated in Fig. 4, comparison of calculated and experimental ECD spectra demonstrated that the calculated ECD curves for (1″*R*,2″*S*,3″*S*,4″*S*,5″*R*,6″*R*,10″*S*)-**1** aligned well with the experimental results. Consequently, the structure of compound **1** (dryatraol J) was conclusively determined, with the absolute configuration assigned as 1″*R*, 2″*S*, 3″*S*, 4″*S*, 5″*R*, 6″*R*, 10″*S*.

The molecular formulas of compounds **2** and **3** were determined to be $C_{35}H_{44}O_9$ and $C_{36}H_{46}O_9$ based on the HRE-SI-MS ion peaks at m/z 609.3064 $[M + H]^+$ (Calcd. for $C_{35}H_{45}O_9$, 609.3058) and m/z 623.3214 $[M + H]^+$ (Calcd. for $C_{36}H_{47}O_9$, 623.3215), respectively. Comparison of the 1D NMR data of **2** and **3** with those of **1** indicated that they shared the same skeletal core, with the only difference being the replacement of the acetyl group (δ_C 202.7 and 30.6) in **1** by a propionyl group (δ_C 205.9, 36.0 and 8.6) in **2** and a butyryl group (δ_C 205.7, 44.6, 18.9, 14.3) in **3**, respectively. These findings were confirmed by the HMBC correlation from H_3-9′ (δ_H 1.15) to C-7′ (δ_C 205.9), along with ^1H-^1H COSY cross-peaks of H_2-8′ (δ_H 3.03) and H_3-9′ in **2**, and HMBC correlation from H_2-8′ (δ_H 2.96) to C-7′ (δ_C 205.7), as well as the ^1H-^1H COSY correlations of H_2-9′ (δ_H 1.70) and H_2-8′/H_3-10′ (δ_H 0.98) in **3**. Consequently, the 2D structures of **2** and **3** were established, and their absolute configurations were determined to be identical to that of **1** due to structural similarities and matching experimental ECD spectra as shown in Fig. 4.

Compound **4** exhibited a molecular formula of $C_{35}H_{42}O_9$, as established by its ^{13}C NMR and HR-ESI-MS data (m/z 605.2761 $[M - H]^-$, Calcd. for $C_{35}H_{41}O_9$, 605.2756). Careful comparison of the 1D NMR data indicated that **4** possessed an identical acylphloroglucinol motif (fragment Ⅰ) to that of compound **2** and the same sesquiterpenoid moiety (fragment Ⅱ) as dryatraol A [9]. The coupling pattern of a furan ring was further confirmed by HMBC correlations from H-1″ (δ_H 5.10) to C-4′ (δ_C 161.7) and from H-2″ (δ_H 3.22) to C-4′/C-5′ (δ_C 114.5). The relative configuration of **4** was determined to be the same as that of dryatraol A, supported by NOE correlations between H_3-14″ (δ_H 1.08) and H-6″ (δ_H 2.36)/H_3-15″ (δ_H 0.98), between H-2″ (δ_H 3.22) and H-4″ (δ_H 2.77), as well as between H_3-13″ (δ_H 1.17) and H-1″ (δ_H 5.10)/H-4″. Comparison of the experimental ECD spectrum with calculated spectra (Fig. 4) led to the assignment of the absolute configuration of compound **4** as 1″*R*, 2″*S*, 4″*S*, 5″*S*, 6″*S*. Consequently, the structure of **4** was determined as depicted.

The HR-ESI-MS spectra of compounds **5** and **6** revealed ion peaks at m/z 591.2626 $[M - H]^-$ (Calcd. for $C_{34}H_{39}O_9$, m/z 591.2600) and m/z 619.2907 $[M - H]^-$ (Calcd. for $C_{36}H_{43}O_9$, 619.2913), respectively, corresponding to their molecular formulas of $C_{34}H_{40}O_9$ and $C_{36}H_{44}O_9$. This indicates that **5** and **6** differ from **4** by fourteen (CH_2) mass units less and more, respectively. Detailed analysis of the 1D NMR data of **5** and **6** revealed close similarity to those of **4**, with the exception of an acetyl unit (δ_C 202.9, 30.8) in **5** and a butyryl group (δ_C 206.2, 44.7, 19.5, 14.3) in **6** replacing the propionyl group in **4**, respectively. The HMBC correlations from H_3-8′ (δ_H 2.56) to C-3′ (δ_C 101.8)/C-7′ (δ_C

202.9) in compound **5**, and ^{1}H-^{1}H COSY spin system of H_2-8′–H_2-9′–H_3-10′ (δ_H 0.94), along with HMBC correlation from H_2-8′ (δ_H 2.87, 2.96) to C-7′ (δ_C 206.2) in compound **6** further confirmed these conclusions. Thus, the planar structures of compounds **5** and **6** were elucidated, and their absolute configurations were determined to be identical to that of **4**, as further evidenced by comparison of their experimental ECD spectra (Fig. 4).

A molecular formula of $C_{26}H_{34}O_5$ was assigned to compound **7** based on the ^{13}C NMR (Table 2) and HRESIMS data. Detailed analysis of the 1D and 2D NMR data of compound **7** revealed the

Table 1 ^{1}H and ^{13}C NMR data for compounds **1**–**4** (J in Hz)[a]

No.	1		2		3		4	
	δ_H	δ_C	δ_H	δ_C	δ_H	δ_C	δ_H	δ_C
1	-	188.0	-	188.0	-	188.1	-	188.0
2	-	108.9	-	109.0	-	109.1	-	109.0
3	-	199.5	-	198.3	-	199.6	-	199.5
4	-	44.7	-	44.6	-	44.8	-	44.8
5	-	172.2	-	172.0	-	172.4	-	172.3
6	-	111.8	-	111.7	-	111.9	-	111.9
7	3.51 s	17.0	3.53 s	17.0	3.53 s	17.2	3.50 s	17.1
8	1.46 s	24.7	1.47 s	24.7	1.47 s	24.8	1.48 s	25.0
9	1.48 s	25.0	1.50 s	25.0	1.49 s	25.1	1.49 s	25.0
10	-	203.9	-	203.5	-	204.0	-	203.9
11	2.69 s	29.2	2.72 s	29.4	2.70 s	29.2	2.70 s	29.4
1′	-	106.7	-	106.7	-	107.0	-	106.6
2′	-	160.5	-	160.0	-	160.6	-	160.0
3′	-	101.5	-	101.0	-	101.3	-	101.4
4′	-	161.0	-	160.8	-	161.0	-	161.7
5′	-	113.9	-	113.9	-	114.0	-	114.5
6′	-	160.6	-	160.0	-	160.9	-	160.3
7′	-	202.7	-	205.9	-	205.7	-	206.3
8′	2.56 s	30.6	3.03 m	36.0	2.96 m	44.6	3.01 m	36.0
9′			1.15 t (7.2)	8.6	1.70 m	18.9	1.11 t (7.3)	8.6
10′					0.98 t (7.4)	14.3		
11′								
12′								
13′								
14′								
15′								
1″	4.28 d (7.8)	91.9	4.28 d (7.8)	91.9	4.28 d (7.8)	92.1	5.10 d (6.4)	89.2
2″	3.49	34.3	3.51 d (7.8)	34.2	3.51 d (7.8)	34.3	3.22 m	38.8
3″	0.52 d (10.1)	25.2	0.53 d (10.1)	25.2	0.52 d (10.1)	25.3	a 1.79 m, b 1.18	33.7
4″	0.49 d (10.1)	34.6	0.50 d (10.1)	34.6	0.50 d (10.1)	34.7	2.77 m	32.0
5″	-	40.3	-	40.3	-	40.5	-	40.3
6″	2.32 m	33.1	2.35 m	33.1	2.33 m	33.2	2.36 d (6.5)	52.3
7″	1.41	30.3	1.43	30.4	1.44	30.5	5.90 dd (9.4, 6.6)	132.2
8″	a 1.95 m, b 1.56 m	20.1	a 1.98 m, b 1.59 m	20.1	a 1.97 m, b 1.56 m	20.2	6.03 dd (9.4, 5.1)	123.4
9″	1.41	32.9	1.43	32.8	1.44	32.9	6.18 d (5.1)	129.1
10″	-	70.5	-	70.4	-	70.6	-	140.7
11″	-	21.7	-	21.7	-	21.8	-	75.7
12″	1.02 s	33.4	1.03 s	33.4	1.03 s	33.5	1.24 s	31.7
13″	1.49 s	17.5	1.50 s	17.5	1.50 s	17.5	1.17 s	25.8
14″	1.08 s	21.1	1.09 s	21.2	1.10 s	21.2	1.08 s	18.7
15″	0.87 d (6.9)	15.8	0.88 d (7.0)	158	0.88 d (7.0)	15.8	0.98 d (6.3)	18.1
3-OH	18.51 s		18.53 s		18.53 s		18.55 s	
5-OH	9.91 s		9.97 s		9.97 s		9.99 s	
7-OH								
2′-OH	15.33 s		15.49 s		15.58 s		15.48 s	
6′-OH	11.30 s		11.29 s		11.20 s		11.22 s	

[a] Measured at 500 (^{1}H) and 125 (^{13}C) MHz in acetone-d_6:$CDCl_3$:TFA (3∶1∶0.01); Overlapped signals are reported without designating multiplicity.

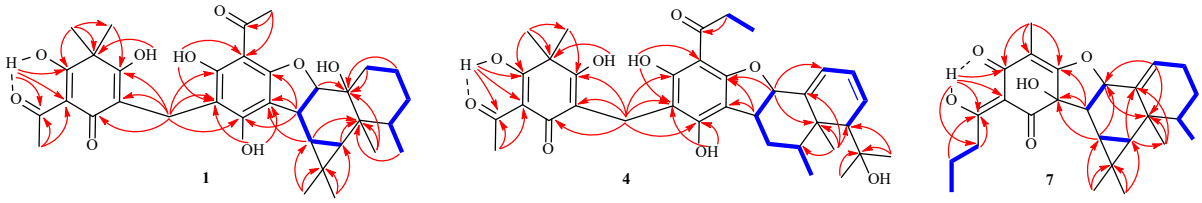

Fig. 2 Key ^{1}H–^{1}H COSY and HMBC correlations of compounds **1**, **4** and **7**.

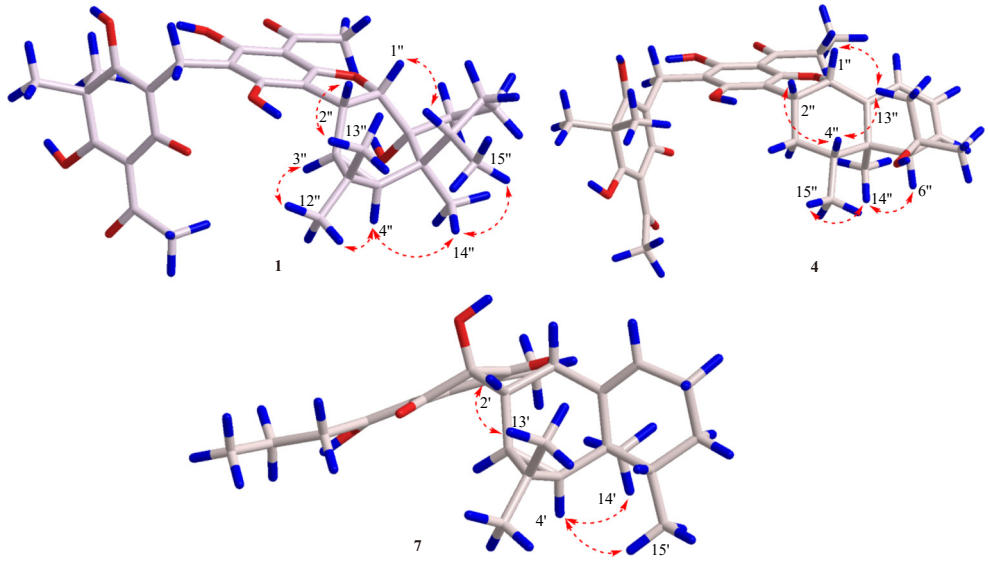

Fig. 3 Key NOESY correlations of compounds **1**, **4** and **7**.

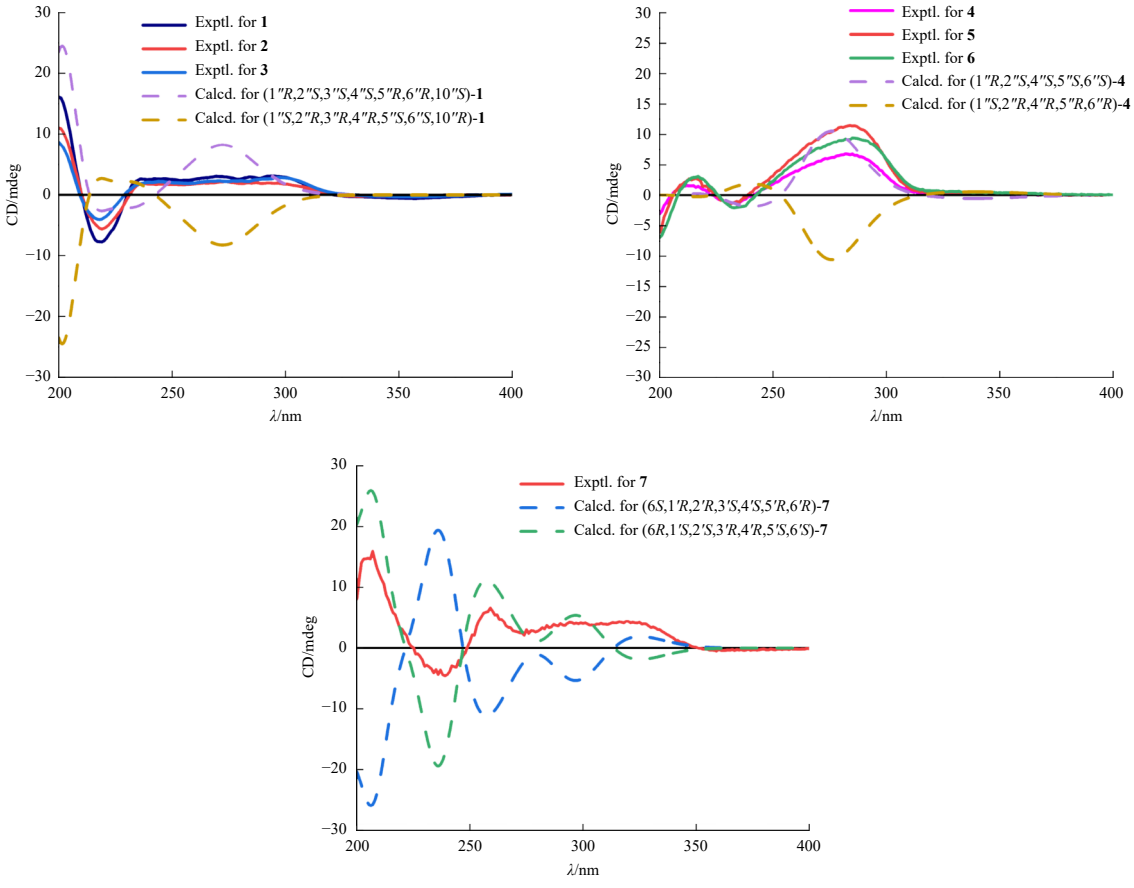

Fig. 4 Experimental and calculated ECD spectra for compounds **1**–**7**.

Table 2 ^{1}H and ^{13}C NMR data for compounds **5**–**7** (*J* in Hz)

No.	**5**[a]		**6**[a]		**7**[b]	
	δ_H	δ_C	δ_H	δ_C	δ_H	δ_C
1	-	188.0	-	188.1	-	191.5
2	-	109.1	-	109.1	-	106.3
3	-	198.4	-	199.7	-	193.6
4	-	44.6	-	44.7	-	104.8
5	-	172.0	-	172.4	-	170.4
6	-	111.8	-	111.9	-	80.7
7	3.51 s	17.0	3.51 s	17.2	-	201.7
8	1.47 s	24.9	1.48 s	24.9	3.01 m	40.8
9	1.47 s	24.9	1.48 s	25.0	1.68	19.0
10	-	203.6	-	204.1	1.01 t (7.0)	14.2
11	2.69 s	29.4	2.69 s	29.2	1.88 s	7.8
1′	-	106.3	-	106.7	5.19 br s	89.8
2′	-	159.6	-	160.2	2.65 br s	43.9
3′	-	101.8	-	101.5	0.14 d (8.9)	17.6
4′	-	162.1	-	161.8	0.61 d (8.9)	32.8
5′	-	114.5	-	114.6	-	34.7
6′	-	159.9	-	160.7	1.68	36.7
7′	-	202.9	-	206.2	1.50 m	26.7
8′	2.56 s	30.8	a 2.87 m, b 2.96 m	44.7	a 2.15 m, b 2.10 m	26.1
9′			1.64 m	19.5	5.89 br s	133.3
10′			0.94 t (7.3)	14.3	-	137.7
11′					-	18.5
12′					0.97 s	16.3
13′					1.01 s	29.4
14′					1.09 s	24.5
15′					0.97	15.7
1″	5.09 d (6.4)	89.2	5.09 d (6.4)	89.2		
2″	3.21 m	38.8	3.22 m	38.8		
3″	a 1.78 m, b 1.19	33.7	a 1.78 m, b 1.18	33.9		
4″	2.75 m	32.0	2.76 m	32.1		
5″	-	40.3	-	40.4		
6″	2.36 d (6.5)	52.2	2.37 d (6.5)	52.3		
7″	5.89 dd (9.5, 6.7)	132.2	5.90 dd (9.6, 6.7)	132.3		
8″	6.02 dd (9.5, 5.1)	123.3	6.03 dd (9.7, 5.1)	123.4		
9″	6.17 d (5.0)	129.2	6.18 d (5.0)	129.2		
10″	-	140.7	-	140.8		
11″	-	75.5	-	75.7		
12″	1.24 s	31.6	1.24 s	31,7		
13″	1.17 s	25.7	1.18 s	25.8		
14″	1.07 s	18.6	1.08 s	18.7		
15″	0.97 d (6.3)	18.1	0.98 d (6.3)	18.1		
3-OH	18.53 s		18.54 s			
5-OH	9.94 s		9.99 s			
7-OH					19.25 s	
2′-OH	15.35 s		15.53 s			
6′-OH	11.22 s		11.22 s			

[a] Measured at 500 (^{1}H) and 125 (^{13}C) MHz in acetone-d_6 : $CDCl_3$: TFA (3 : 1 : 0.01); [b] Measured at 500 (^{1}H) and 125 (^{13}C) MHz in $CDCl_3$; Overlapped signals are reported without designating multiplicity.

presence of a sesquiterpenoid moiety (fragment Ⅱ) similar to that of compound **1**, with the exception that the hydroxyl group at C-10″ in compound **1** was eliminated to form a C-9′–C-10′ double bond in compound **7**. This observation was corroborated by the 2D NMR correlations as illustrated in Fig. 2. The remaining substructure, a monomeric acylphloroglucinol moiety (fragment Ⅰ) analogous to compound Ⅸ [12], was elucidated through ^{1}H-^{1}H COSY and HMBC correlations. The HMBC cross peaks between the hydrogen-bonded hydroxyl of HO-7 (δ_H 19.25) and C-2 (δ_C 106.3)/C-3 (δ_C 193.6)/C-7 (δ_C 201.7)/C-8 (δ_C 40.8), along with the correlation between H_2-8 (δ_H 3.01) and C-7, and the ^{1}H-^{1}H COSY correlations of H_2-8–H_2-9–H_3-10 (δ_H 1.01) indicated that the hydrogen-bonded hydroxyl and butyryl groups were attached at C-7 and C-2, respectively. Furthermore, the correlations from H_3-11 (δ_H 1.88) to C-3/C-4 (δ_C 104.8)/C-5 (δ_C 170.4) observed in the HMBC spectrum, and a reduced signal for a methyl compared to compound Ⅸ, revealed that C-6 (δ_C 80.7) was fused with fragment Ⅱ. The remaining fused positions of C-5/C-1′/C-2′ were supported by the HMBC correlations from H-2′ (δ_H 2.65) to C-5/C-6, and the ^{1}H-^{1}H COSY correlation between H-1′ (δ_H 5.19) and H-2′. In conjunction with the analyses of carbon chemical shift values for C-1′ (δ_C 89.8)/C-5 (δ_C 170.4) and molecular information, the linkages of C-1′–O–C-5 and C-2′–C-6 were established, constructing a furan ring. Consequently, the 2D structure of **7** was determined.

The partial relative chiral traits of fragment Ⅱ in **7** were determined through NOESY spectrum analysis (Fig. 3). NOE correlations between H-2′ (δ_H 2.65) and H_3-13′ (δ_H 1.01), as well as H-4′ (δ_H 0.61) and H_3-14′ (δ_H 1.09)/H_3-15′ (δ_H 0.97) indicated that the sesquiterpenoid moiety possessed the same relative stereochemistry as compound **1**. However, no valid NOE signals were available to elucidate the relative configurations of HO-6 and H-1′. To ascertain the relative configuration of the entire structure of **7**, theoretical calculations of ^{13}C NMR shifts for four plausible relative structures of **7** (**7a**–**7d**, Fig. 5) were conducted at the mpw1pw 91/6-311g (d, p) level in $CDCl_3$. The correlation coefficient (R^2) results for **7a**–**7d** were 0.9953, 0.9913, 0.9972, and 0.9986, respectively, suggesting that **7d** was the most probable relative structure. To further verify this conclusion, ^{13}C NMR-DP4+ probability analysis was performed on the four structures (**7a**–**7d**), confirming **7d** as the correct structure with an overall DP4+ probability of 100% (Fig. 6). Finally, comparison between the experimental ECD spectrum of **7** and the calculated spectra of two individual enantiomers of **7d** determined the absolute configuration of **7** as 6*R*, 1′*S*, 2′*S*, 3′*R*, 4′*R*, 5′*S*, 6′*S*.

Considering that phloroglucinols isolated from the genus *Dryopteris* [4, 9, 13-16] have demonstrated significant antiviral activities, all isolates were evaluated for their antiviral efficacy against RSV and HSV-1 using a cytopathic effect inhibition assay. Acyclovir and ribavirin served as positive controls, respectively. The results (Table 3) indicated that all compounds exhibited substantial anti-RSV and anti-HSV-1 activities. Notably, compounds **1**–**6** demonstrated more potent anti-RSV activities compared to the positive control (ribavirin), with IC_{50} values ranging from 0.75 to 3.12 μmol·L^{-1}.

Phloroglucinols are considered the primary effective and characteristic constituents of *Dryopteris* plants, with acylphloroglucinol-terpenoid adducts garnering significant attention. This study reports the isolation of seven novel acylphloroglucinol-sesquiterpenoid adducts, designated as dryatraols J–P (**1**–**7**), from the rhizomes of *Dryopteris atrata*. Structural elucidation was accomplished using MS, NMR spectroscopic data, and quantum

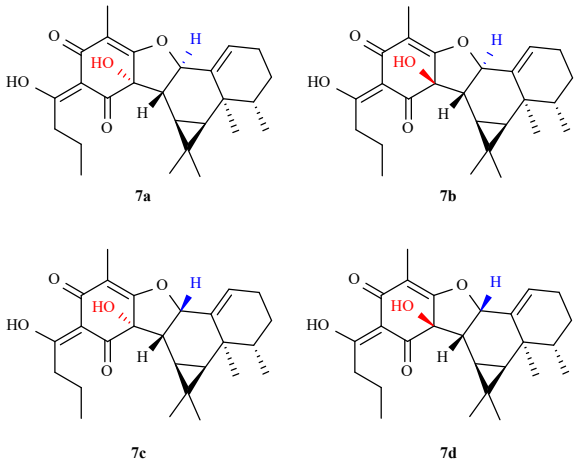

Fig. 5 Four proposed relative structures of **7**.

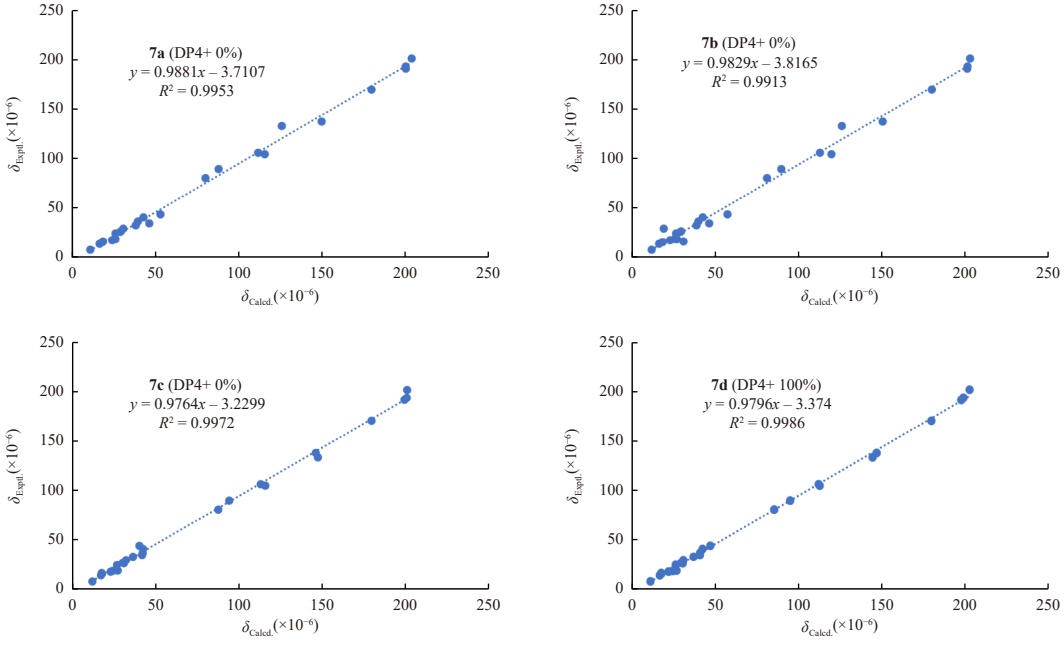

Fig. 6 Correlation coefficients and DP4+ probability analyses between the calculated and experimental ^{13}C NMR chemical shifts for **7a**–**7d**.

Table 3 Anti-RSV and anti-HSV-1 activities (mean ± SD, n = 3)

Compounds	RSV			HSV-1		
	CC_{50} (μmol·L^{-1})	IC_{50} (μmol·L^{-1})	SI	CC_{50} (μmol·L^{-1})	IC_{50} (μmol·L^{-1}	SI
1	59.80 ± 4.82	0.75 ± 0.12	79.73	20.90 ± 2.27	3.75 ± 1.02	5.57
2	50.09 ± 1.36	0.75 ± 0.09	66.78	20.77 ± 5.95	3.75 ± 0.54	5.53
3	60.00 ± 3.74	1.56 ± 0.37	38.46	20.00 ± 4.17	5.00 ± 0.81	4.00
4	> 100	1.56 ± 0.20	> 64.10	50.53 ± 3.56	9.38 ± 0.78	5.38
5	> 100	3.12 ± 0.34	> 32.05	100.00 ± 8.17	12.50 ± 2.04	8.00
6	> 100	1.56 ± 0.13	> 64.10	50.00 ± 5.33	9.38 ± 1.34	5.33
7	> 100	25.00 ± 1.63	> 4.00	> 100	25.00 ± 2.45	> 4.00
Acyclovir				> 100	1.25 ± 0.12	> 80.00
Ribavirin	> 100	6.25 ± 1.27	> 16.00			

IC_{50} is the concentration of compound that reduced 50% cytopathic effect as compared to that of control cells infected with RSV/HSV-1. CC_{50} is the concentration of compound with half maximal inhibition on the growth and survival of the host cells. SI means CC_{50}/IC_{50}.

chemical calculations. These structures represent a less common subclass of carbon architecture in acylphloroglucinol-sesquiterpenoid adducts, featuring a furan ring as the linkage, thereby enhancing the chemical diversity of phloroglucinols produced by *Dryopteris* plants. Compounds **1**–**6** are the first reported instances of acylphloroglucinol-sesquiterpenoid adducts comprising dimeric acylphloroglucinol and aristolane- or rulepidanol-type sesquiterpene, while compound **7** exhibits a hydroxylated monomeric acylphloroglucinol moiety. Furthermore, compounds **1**–**6** demonstrated superior anti-RSV activities compared to the positive control (ribavirin), warranting further investigation.

3. Experimental

3.1. General experiment procedures

Optical rotations were measured using a JASCO P-1020 polarimeter. High-resolution electrospray ionization mass spectrometry (HR-ESI-MS) data were obtained on an Agilent 6210 LC/MSD TOF mass spectrometer. UV spectra were recorded on a JASCO V-550 UV/*vis* spectrophotometer. 1D and 2D NMR spectra were acquired on a Bruker AV-500 spectrometer (^{1}H: 500 MHz, ^{13}C: 125 MHz) with tetramethylsilane (TMS) as the internal standard. Analytical high-performance liquid chromatography (HPLC) was performed on a Shimadzu LC system equipped with an LC-20AD pump and an SPDM-20A PDA detector, utilizing a Cosmosil C_{18} analytical column (5 μm, 4.6 mm × 250 mm). Preparative HPLC was conducted using a Varian Prostar system with a preparative Cosmosil C_{18} column (5 μm, 20 mm × 250 mm). Open column chromatography (CC) was carried out using silica gel (200–300 mesh), octadecylsilane (ODS) (50 μm, 120 Å, YMC), and Sephadex LH-20 (25–100 μm). All reagents used in CC and HPLC were of analytical grade and chromatographic grade, respectively.

3.2. Plant materials

The rhizomes of *D. atrata* were collected in Yunnan Province, China, in September 2019. Prof. Guangxiong Zhou from the College of Pharmacy at Jinan University confirmed the plant's identification. A voucher specimen (No. 2019092601) has been deposited at the Institute of Traditional Chinese Medicine & Natural Products, Jinan University, Guangzhou, China.

3.3. Extraction and isolation

The dried and powdered rhizomes of *D. atrata* (8.0 kg) were extracted four times with 95% ethanol at room temperature (4 × 60.0 L). Following filtration, the solvent was removed under reduced pressure using a rotary evaporator, yielding a crude extract (1.1 kg). This extract was suspended in water (1.0 L) and subsequently partitioned with petroleum ether (3 × 3.0 L). After solvent removal, the entire petroleum ether extract (250.7 g) underwent silica gel CC elution with petroleum ether/ethyl acetate in a gradient (100∶0 to 0∶100, *V*/*V*), resulting in seven fractions (Fr. A to Fr. G). Fr. D (20.7 g) was further purified using an ODS CC with a stepwise gradient solvent system of MeOH/H_2O (60∶40 to 100∶0, *V*/*V*), producing four subfractions (Fr. D1 to Fr. D4). Fr. D4 (4.6 g) was then subjected to silica gel CC using a gradient elution of *n*-hexane/ethyl acetate (50∶1 to 5∶1) , yielding four subfractions (Fr. D4a to Fr. D4d). Compounds **1** (10.2 mg, t_R 27.0 min), **2** (6.2 mg, t_R 35.2 min) and **3** (5.0 mg, t_R 39.3 min) were isolated from Fr. D4c (0.3 g) by preparative HPLC [MeOH/H_2O (0.1% TFA), 98∶2, *V*/*V*]. Fr. D2 (2.4 g) was subjected to a Sephadex LH-20 column and eluted with CH_2Cl_2/MeOH (1∶1, *V*/*V*), resulting in three additional fractions (Fr. D2a to Fr. D2c). Fr. D2b (0.2 g) was separated by semipreparative HPLC [MeOH/H_2O (0.1% HCOOH), 85∶15, *V*/*V*] to yield **7** (3.5 mg, t_R 20 min). Fr. B (20.6 g) was loaded on an ODS CC and purified with a step gradient solvent of MeOH/H_2O (60:40 to100∶0, *V*/*V*) to afford four subfractions (Fr. B1 to Fr. B4). Fr. B4 (4.2 g) was then subjected to silica gel CC eluted with *n*-hexane/ethyl acetate in a gradient (60∶1 to 5∶1) and divided into three parts (Fr. B4a to Fr. B4c). Compounds **4** (9.2 mg, t_R 37 min), **5** (4.2 mg, t_R 44 min) and **6** (8.0 mg, t_R 29 min) were obtained from Fr. B4b (0.3 g) using preparative HPLC [MeOH/H_2O (0.1% TFA), 98∶2, *V*/*V*].

3.4. Spectroscopic data of compounds

Dryatraol J (**1**): yellow oil; $[\alpha]_D^{25}$ +43.2 (*c* 0.1, CH_3CN); UV (CH_3CN) λ_{max} 231, 288 nm; IR (KBr) ν_{max} 3496, 2930, 2877, 1638, 1534, 1451, 1374, 1260, 1197, 1142, 1012, 910, 728, 608 cm^{-1}; ^{1}H and ^{13}C NMR data see Table 1; HR-ESI-MS *m*/*z* 595.2895 [M + H]$^+$ (Calculated for $C_{34}H_{43}O_9$, 595.2902).

Dryatraol K (**2**): yellow oil; $[\alpha]_D^{25}$ +51.4 (*c* 0.1, CH_3CN); UV (CH_3CN) λ_{max} 231, 288 nm; IR (KBr) ν_{max} 3515, 2930, 2870, 1638, 1534, 1469, 1448, 1372, 1316, 1260, 1137, 1086, 910, 733 cm^{-1}; ^{1}H and ^{13}C NMR data see Table 1; HR-ESI-MS *m*/*z* 609.3064 [M +

H]$^+$ (Calculated for $C_{35}H_{45}O_9$, 609.3058).

Dryatraol L (**3**): yellow oil; $[\alpha]_D^{25}$ +47.3 (*c* 0.1, CH_3CN); UV (CH_3CN) λ_{max} 231, 288 nm; IR (KBr) ν_{max} 3406, 2935, 2867, 2858, 1634, 1534, 1464, 1446, 1367, 1314, 1258, 1139, 1017, 915, 738 cm^{-1}; ^{1}H and ^{13}C NMR data see Table 1; HR-ESI-MS *m/z* 623.3214 [M + H]$^+$ (Calculated for $C_{36}H_{47}O_9$, 623.3215).

Dryatraol M (**4**): orange oil; $[\alpha]_D^{25}$ +23.2 (*c* 0.2, CH_3CN); UV (CH_3CN) λ_{max} 231, 286 nm; IR (KBr) ν_{max} 3443, 2963, 2930, 1629, 1439, 1378, 1200, 1103, 1068, 1019, 810, 715 cm^{-1}; ^{1}H and ^{13}C NMR data see Table 1; HR-ESI-MS *m/z* 605.2761 [M − H]$^-$ (Calculated for $C_{35}H_{41}O_9$, 605.2756).

Dryatraol N (**5**): orange oil; $[\alpha]_D^{25}$ +34.8 (*c* 0.2, CH_3CN); UV (CH_3CN) λ_{max}: 231, 286 nm; IR (KBr) ν_{max}: 3454, 2938, 1634, 1434, 1380, 1195, 1109, 1024, 794, 725 cm^{-1}; ^{1}H and ^{13}C NMR data see Table 2; HR-ESI-MS *m/z* 591.2626 [M − H]$^-$ (Calculated for $C_{34}H_{39}O_9$, 591.2600).

Dryatraol O (**6**): orange oil; $[\alpha]_D^{25}$ +31.7 (*c* 0.3, CH_3CN); UV (CH_3CN) λ_{max} 231, 286 nm; IR (KBr) ν_{max} 3441, 2933, 1629, 1441, 1376, 1197, 1134, 1105, 1028, 806, 717 cm^{-1}; ^{1}H and ^{13}C NMR data see Table 2; HR-ESI-MS *m/z* 619.2907 [M − H]$^-$ (Calculated for $C_{27}H_{41}O_5$, 619.2913).

Dryatraol P (**7**): yellow gum; $[\alpha]_D^{25}$ +27.8 (*c* 0.1, MeOH); UV (MeOH) λ_{max}: 200, 249, 290 nm; IR (KBr) ν_{max}: 3441, 2926, 2865, 1629, 1441, 1376, 1276, 1772, 1079, 824, 608 cm^{-1}; ^{1}H and ^{13}C NMR data see Table 2; HR-ESI-MS *m/z* 427.2486 [M + H]$^+$ (Calculated for $C_{26}H_{35}O_5$, 427.2479).

3.5. Computation ECD and NMR methods

The theoretical computation of ECD and NMR spectra, along with the generation of corresponding calculated ECD spectra, adhered to the previously described methodology [4, 17]. Detailed information regarding this process is provided in the supplementary material.

3.6. In vitro anti-viral assay

The antiviral activities of all isolated compounds were evaluated *in vitro* against RSV and HSV-1 using the cytopathic effect reduction assay. Further details regarding this methodology can be found in our previous publications [4, 9].

Funding

This work was supported by the National Natural Science Foundation of China (Nos. 82173695, 82003609 and 82003743), the Guangdong Basic and Applied Basic Research Foundation (Nos. 2023A1515011896 and 2020A1515110453), the Science and Technology Planning Project of Guangzhou City (No. 2023A03J0566), and the High-performance Public Computing Service Platform of Jinan University.

Declaration of competing interest

These authors have no conflict of interest to declare.

References

1 Celaj O, Durán AG, Cennamo P, et al. Phloroglucinols from Myrtaceae: attractive targets for structural characterization, biological properties and synthetic procedures. *Phytochem Rev*. 2021;20:259-299. https://doi.org/10.1007/s11101-020-09697-2.
2 Singh IP, Bharate SB. Phloroglucinol compounds of natural origin. *Nat Prod Rep*. 2006;23:558-591. https://doi.org/10.1039/b600518g.
3 Han X, Li Z, Li CY, et al. Phytochemical constituents and biological activities of plants from the genus *Dryopteris*. *Chem Biodivers*. 2015;12:1131-1162. https://doi.org/10.1002/cbdv.201400157.
4 Chen NH, Wu ZN, Li W, et al. Acylphloroglucinols-based meroterpenoid enantiomers with antiviral activities from *Dryopteris crassirhizoma*. *Ind Crop Prod*. 2020;150:112415-112423. https://doi.org/10.1016/j.indcrop.2020.112415.
5 Hai P, Rao KR, Jiang N, et al. Structure elucidation, biogenesis, and bioactivities of acylphloroglucinol-derived meroterpenoid enantiomers from *Dryopteris crassirhizoma*. *Bioorg Chem*. 2022;119:105567-105579. https://doi.org/10.1016/j.bioorg.2021.105567.
6 Hai P, He YQ, Wang RR, et al. New tocopherol and acylphloroglucinol derivatives from *Dryopteris crassirhizoma* and their antimicrobial activities. *Fitoterapia*. 2023;165:105401-105409. https://doi.org/10.1016/j.fitote.2022.105401.
7 Hai P, He YQ, Wang RR, et al. Antimicrobial acylphloroglucinol meroterpenoids and acylphloroglucinols from *Dryopteris crassirhizoma*. *Planta Med*. 2023;89(3):295-307. https://doi.org/10.1055/a-1917-7910.
8 Chen NH, Zhang YB, Huang XJ, et al. Drychampones A–C: three meroterpenoids from *Dryopteris championii*. *J Org Chem*. 2016;81(19):9443-9448. https://doi.org/10.1021/acs.joc.6b01720.
9 Zhang JH, Chen JL, Xu WB, et al. Undescribed phloroglucinol derivatives with antiviral activities from *Dryopteris atrata* (Wall. Ex Kunze) Ching. *Phytochemistry*. 2023;208:113585-113594. https://doi.org/10.1016/j.phytochem.2023.113585.
10 Hou B, Liu Z, Yang XB, et al. Total synthesis of dryocrassin ABBA and its analogues with potential inhibitory activity against drug-resistant neuraminidases. *Bioorg Med Chem*. 2019;27(17):3846-3852. https://doi.org/10.1016/j.bmc.2019.07.013.
11 Ji NY, Li XM, Ding LP, et al. Two new aristolane sesquiterpenes from *Laurencia similis*. *Chin Chem Lett*. 2007;18(2):178-180. https://doi.org/10.1016/j.cclet.2006.12.043.
12 Äyräs P, Lötjönen S, Widén CJ. NMR spectroscopy of naturally occurring phloroglucinol derivatives. *Planta Med*. 1981;42:187-194. https://doi.org/10.1055/s-2007-971624.
13 Maryam M, Te KK, Wong FC, et al. Antiviral activity of traditional Chinese medicinal plants *Dryopteris crassirhizoma* and *Morus alba* against dengue virus. *J Integr Agr*. 2020;19(4):1085-1096. https://doi.org/10.1016/S2095-3119(19)62820-0.
14 Jin YH, Jeon S, Lee J, et al. Anticoronaviral activity of the natural phloroglucinols, dryocrassin ABBA and filixic acid ABA from the rhizome of *Dryopteris crassirhizoma* by targeting the main protease of SARS-CoV-2. *Pharmaceutics*. 2022;14(2):376-386. https://doi.org/10.3390/pharmaceutics14020376.
15 Hou B, Zhang YM, Liao HY, et al. Target-based virtual screening and LC/MS-guided isolation procedure for identifying phloroglucinol-terpenoid inhibitors of SARS-CoV-2. *J Nat Prod*. 2022;85(2):327-336. https://doi.org/10.1021/acs.jnatprod.1c00805.
16 Wang J, Yan YT, Fu SZ, et al. Anti-influenza virus (H5N1) activity screening on the phloroglucinols from rhizomes of *Dryopteris crassirhizoma*. *Molecules*. 2017;22(3):431-446. https://doi.org/10.3390/molecules22030431.
17 Zhang JY, Liu F, Jin Q, et al. Discovery of unusual phloroglucinol–triterpenoid adducts from *Leptospermum scoparium* and *Xanthostemon chrysanthus* by building blocks-based molecular networking. *Chin Chem Lett*. 2023;34:108881-108888. https://doi.org/10.1016/j.cclet.2023.108881.